



# Radiative transfer in a discrete random medium adjacent to a half-space with a rough interface

Adrian Doicu<sup>a,\*</sup>, Michael I. Mishchenko<sup>b</sup>

<sup>a</sup>Deutsches Zentrum für Luft- und Raumfahrt (DLR), Institut für Methodik der Fernerkundung (IMF), Oberpfaffenhofen 82234, Germany

<sup>b</sup>NASA Goddard Institute for Space Studies, 2880 Broadway, New York, NY 10025, USA



## ARTICLE INFO

### Article history:

Received 4 June 2018

Revised 23 July 2018

Accepted 23 July 2018

Available online 24 July 2018

### Keywords:

Electromagnetic scattering

Frequency-domain macroscopic

electromagnetics

Discrete random media

Rough interfaces

Radiative transfer theory

## ABSTRACT

For a macroscopically plane-parallel discrete random medium, the boundary conditions for the specific coherency dyadic at a rough interface are derived. The derivation is based on a modification of the Twersky approximation for a scattering system consisting of a group of particles and the rough surface, and reduces to the solution of the scattering problem for a rough surface illuminated by a plane electromagnetic wave propagating in a discrete random medium with non-scattering boundaries. In a matrix-form setting, the boundary conditions for the specific coherency dyadic imply the boundary conditions for specific intensity column vectors which in turn, yield the expressions for the reflection and transmission matrices. The derived expressions are shown to be identical to those obtained by applying a phenomenological approach based on a facet model to the solution of the scattering problem for a rough surface illuminated by a plane electromagnetic wave.

© 2018 Elsevier Ltd. All rights reserved.

## 1. Introduction

The main goal of a radiative transfer model for a discrete random medium (as defined in Ref. [1]), confined to a layer with rough optical interfaces as its boundaries is the derivation of equations describing the electromagnetic energy budget of a finite volume of space or the reading of a specific detector of electromagnetic energy flow such as a well-collimated radiometer [2,3]. This is usually accomplished by arriving, in the final analysis, at a transport-type equation for the specific coherency dyadic  $\overline{\Sigma}$  (defined through the angular spectrum of the coherency dyadic  $\overline{\mathbf{C}}$ ).

The procedure adopted in Ref. [4–6] is to write the Maxwell equations in an integral form with the help of Green functions and apply the Wigner transform to the equation thus derived. Then, by differentiating this equation, the transport equation is obtained. The coupling between the random medium and the rough boundaries is described through the scattering operators of the rough surfaces. Boundary conditions for  $\overline{\Sigma}$  at the rough interfaces are added to the transport equation in order to guarantee the uniqueness of solution. In particular, the boundary conditions are obtained from the integral equations for the specific coherency dyadics in the upward and downward directions written at the average planes of the rough surfaces. The transport equation for a

sparse discrete random layer is obtained by specializing the results for dense media, i.e., by assuming that the particle concentration is low and the positions of the particles are uncorrelated. In this case, the matrix form representation of the transport equation for  $\overline{\Sigma}$  is analogous to the vector radiative transfer equation for the specific intensity column vector  $\mathbf{I}$ , while the boundary conditions coincide with those for dense media. The main weakness of the approach in Refs. [4–6] is that it is based on the phenomenological postulation of the so-called quasi-uniform field approximation [7]. This allows for the use of the Wigner transform, but amounts to making *a priori* assumptions about the random electromagnetic field rather than specific macro- and microphysical assumptions about the discrete random medium. This makes it problematic (if even possible) to establish definitively the physical meaning of various quantities introduced on an *ad hoc* basis and clarify their relevance to solving the main problem summarized in the first sentence of this section.

A self-consistent radiative transfer theory for sparse discrete random media with non-scattering boundaries, otherwise known as the microphysical radiative transfer theory, has been developed in Refs. [2,8,9]. Taking into account that for sparse media, (i) the particles are widely spaced so that each of them is situated in the far-field region of all the other particles, and (ii) the field (observation) point is situated in the far-field region of all the particles, the far-field Neumann expansion in conjunction with the Twersky approximation is used from the very outset to represent the total field inside the particulate medium. In the rest of the derivation, (i) the coherency dyadic  $\overline{\mathbf{C}}$  is computed under the

\* Corresponding author.

E-mail address: [adrian.doicu@dlr.de](mailto:adrian.doicu@dlr.de) (A. Doicu).

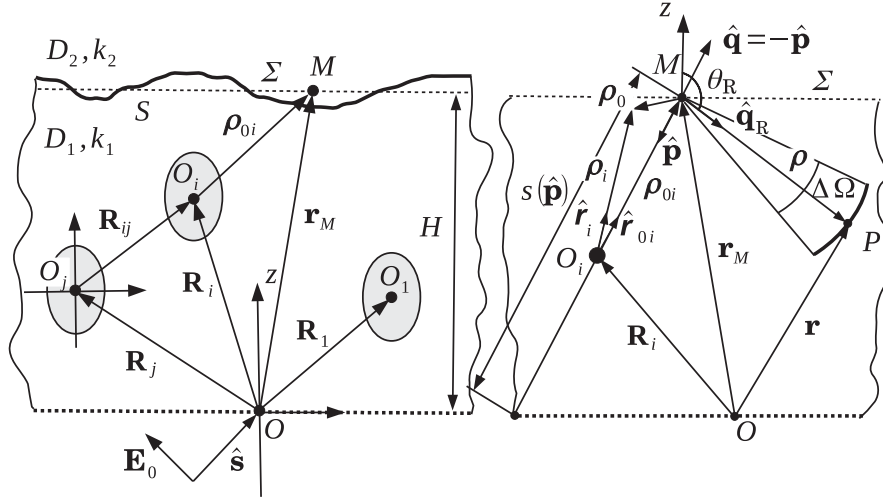


**Fig. 1.** Left: scattering geometry of a discrete random layer with a non-scattering lower plane boundary  $z = 0$  and an upper rough surface boundary  $S$ . Right: local coordinate system attached to  $M$ .

ladder approximation, (ii) an order-of-scattering expansion for the specific coherency dyadic  $\bar{\Sigma}$  is derived, (iii) the order-of-scattering expansion for  $\bar{\Sigma}$  is cast into an integral equation for  $\bar{\Sigma}$ , and finally, (iv) the integral equation for  $\bar{\Sigma}$  is used to obtain the integral form of the vector radiative transfer equation for  $\mathbf{I}$ .

To the extent that the correspondence with the standard phenomenological transfer equation is demonstrated, the boundary conditions for  $\mathbf{I}$  are then typically obtained by considering a separate problem, namely the scattering by a rough surface illuminated by a plane electromagnetic wave. This specific problem is solved by using either an electromagnetic scattering model [10–12] or an *ad hoc* geometrical-optics approach based on a facet model for the rough surface [13–18]. The reflected and incident specific intensity column vectors as well as the transmitted and incident specific intensity column vectors are related via the reflection and transmission matrices, respectively. The obvious weakness of this phenomenological approach is that it is based on *ad hoc* manipulations with second moments in the electromagnetic field rather than with the field itself.

The goal of this paper is to derive the boundary conditions for the specific coherency dyadic at a rough interface in the case of a sparse discrete random medium by adopting several aspects of the microphysical approach outlined in Refs. [2,8,9]. The derivation is based on a modified Twersky approximation for a scattering system consisting of a group of particles and a rough surface. Essentially, we apply the microphysical approach to solve the scattering problem for a rough surface illuminated by a plane electromagnetic wave propagating in a discrete random medium with non-scattering boundaries. In a matrix-form setting, the boundary conditions for the specific coherency dyadic yield the boundary conditions for the specific intensity column vector, and hence analytical expressions for the reflection and transmission matrices.

## 2. Boundary conditions for the specific coherency dyadic at a rough interface

We consider a system of  $N$  identical homogeneous particles placed in a domain  $D_1$  and centered at  $\mathbf{R}_1, \mathbf{R}_2, \dots, \mathbf{R}_N$  (Fig. 1). For simplicity we assume that the particles have the same orientation and that the particle coordinate system is aligned with the global coordinate system. The origins of the particles are confined to a layer with a non-scattering lower plane boundary  $z = 0$  and an upper rough surface boundary  $S$ . The surface  $S$  separates the non-magnetic domains  $D_1$  and  $D_2$  of wavenumbers  $k_1 = \omega\sqrt{\varepsilon_1\mu_0}$  and

$k_2 = \omega\sqrt{\varepsilon_2\mu_0}$ , respectively, where  $\omega$  is the angular frequency,  $\varepsilon_1$  and  $\varepsilon_2$  are the electric permittivities in domains  $D_1$  and  $D_2$ , respectively, and  $\mu_0$  is the magnetic permeability of a vacuum. The relative refractive index of domain  $D_2$  with respect to domain  $D_1$  is denoted by  $m = k_2/k_1$ . The incident wave illuminating the discrete random layer from below is a plane electromagnetic wave with the direction specified by a unit vector  $\hat{\mathbf{s}}$  and an amplitude  $\mathcal{E}_0(\hat{\mathbf{s}})$ :

$$\mathbf{E}_0(\mathbf{r}) = \mathcal{E}_0(\hat{\mathbf{s}})e^{ik_1\hat{\mathbf{s}}\cdot\mathbf{r}}. \quad (1)$$

Note that we imply and suppress throughout the paper the complex time-harmonic factor  $\exp(-j\omega t)$ , where  $t$  is time. The average plane of the rough surface  $S$  is the plane  $z = H$ , denoted by  $\Sigma$ . If  $M$  is a point on  $\Sigma$ , we let  $M_S$  be the corresponding point on the surface characterized by the random function  $z = H + h(\mathbf{r}_{M\perp})$ , where  $\mathbf{r}_M$  is the position vector of  $M$  and  $\mathbf{r}_{M\perp}$  the transverse component of  $\mathbf{r}_M$ , i.e.,  $\mathbf{r}_M = \mathbf{r}_{M\perp} + (\mathbf{r}_M \cdot \hat{\mathbf{z}})\hat{\mathbf{z}}$ .

### 2.1. Reflection

We consider a downward reflection direction  $\hat{\mathbf{q}}_R = \hat{\mathbf{q}}_R(\theta_R, \varphi_R)$  characterized by the polar and azimuthal angles  $\theta_R$  and  $\varphi_R$ , respectively, with  $\theta_R > \pi/2$ , an elementary solid angle  $\Delta\Omega$  around  $\hat{\mathbf{q}}_R$ , and a field point  $P$  along the direction  $\hat{\mathbf{q}}_R$  situated at a distance  $\rho$  with respect to  $M$  (Fig. 1). The field point  $P$  is specified in the global coordinate system by the position vector  $\mathbf{r}$  and in the local coordinate system attached to  $M$  by the position vector  $\boldsymbol{\rho} = \rho\hat{\mathbf{q}}_R$ .

As the first step of our analysis, we derive a series representation for the specific coherency dyadic in the upward direction  $\hat{\mathbf{q}}$ ,  $\bar{\Sigma}(\mathbf{r}_M, \hat{\mathbf{q}})$ , while as the second step, we relate the specific coherency dyadic in the downward direction  $\hat{\mathbf{q}}_R$ ,  $\bar{\Sigma}(\mathbf{r}_M, \hat{\mathbf{q}}_R)$  to  $\bar{\Sigma}(\mathbf{r}_M, \hat{\mathbf{q}})$ .

**Step 1.** In the Twersky approximation for an isolated group of particles [8,9], only self-avoiding scattering paths (i.e., the paths that go through a scatterer only once) are considered. As a result, the field exciting a particle at a point near the particle is the total field that would exist at that point if the particle were removed from the group. For a scattering system consisting of a group of particles and a rough surface, we use a modified Twersky approximation implying that (i) the field exciting (illuminating) the rough surface is the total field produced by the group of particles in the absence of the rough surface, and (ii) the field scattered by the surface is not scattered by the particles as it propagates at the field point  $P$ . In other words, the total field exciting the rough surface corresponds to a discrete random layer with the

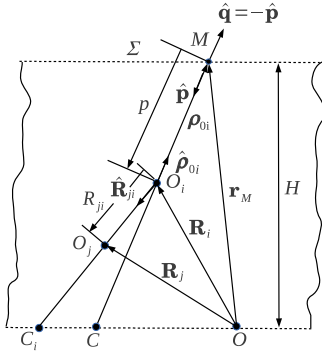


Fig. 2. Geometry for computing the configuration average.

non-scattering boundaries  $z = 0$  and  $z = H$  and being illuminated by a plane electromagnetic wave as in Eq. (1). Furthermore, because our goal is to derive the boundary condition for the specific coherency dyadic, we consider the waves scattered by the surface in an elementary solid angle  $\Delta\Omega$  around  $\hat{\mathbf{q}}_R$  and propagating in a non-scattering medium at  $P$ . It is clear that a scattering model based on the modified Twersky approximation is more comprehensive than the conventional model dealing with the scattering by a rough surface illuminated by a plane electromagnetic wave propagating in free space.

For a discrete random layer with the non-scattering boundaries  $z = 0$  and  $z = H$  and being illuminated by a plane electromagnetic wave given by Eq. (1), the total field at  $M$  (residing on the average plane of the rough surface) is given by

$$\mathbf{E}(\mathbf{r}_M) = \mathbf{E}_0(\mathbf{r}_M) + \sum_i \mathbf{E}_{\text{sct}i}(\mathbf{r}_M). \quad (2)$$

In the standard Twersky approximation for the group of particles, the order-of-scattering expansion for the total field is

$$\begin{aligned} \mathbf{E}(\mathbf{r}_M) = & \mathbf{E}_0(\mathbf{r}_M) + \sum_i \bar{\mathbf{U}}(\rho_{0i}, \hat{\mathbf{s}}) \cdot \mathbf{E}_0(\mathbf{R}_i) \\ & + \sum_i \sum_{j \neq i} \bar{\mathbf{U}}(\rho_{0i}, \hat{\mathbf{R}}_{ij}) \cdot \bar{\mathbf{U}}(\mathbf{R}_{ij}, \hat{\mathbf{s}}) \cdot \mathbf{E}_0(\mathbf{R}_j) + \dots, \end{aligned} \quad (3)$$

where we use the notation of Fig. 2,  $\mathbf{R}_{ij} = \mathbf{R}_i - \mathbf{R}_j$  and

$$\bar{\mathbf{U}}(\rho_{0i}, \hat{\mathbf{q}}) = \frac{e^{jk_1 \rho_{0i}}}{\rho_{0i}} \bar{\mathbf{A}}(\hat{\rho}_{0i}, \hat{\mathbf{q}}) \quad (4)$$

for any incident direction  $\hat{\mathbf{q}}$ . In the above definition of the dyadic  $\bar{\mathbf{U}}$ ,  $\bar{\mathbf{A}}$  is the far-field scattering dyadic [2,9]. A diagrammatic representation of the expansion (3) is

$$\mathbf{E}(\mathbf{r}_M) = \overset{M}{\leftarrow} + \sum_i \overset{M}{\leftarrow} \overset{i}{\circ} \leftarrow + \sum_{i, j \neq i} \overset{M}{\leftarrow} \overset{i}{\circ} \overset{j}{\circ} \leftarrow + \dots, \quad (5)$$

where the symbol  $\leftarrow$  represents the incident field  $\mathbf{E}_0$ , while the composed symbol  $\leftarrow \circ$  denotes multiplying a field by the dyadic  $\bar{\mathbf{U}}$ . In the radiative transfer theory of discrete random media the key quantity is the coherency dyadic. To compute the coherent field, the procedure of configuration averaging based on the assumption of ergodicity and requiring the computation of integrals over particle positions, is considered. To integrate over all positions of particle  $i$  we use a local coordinate system with the origin at  $M$ , to integrate over all positions of particle  $j$  we use a local coordinate system with the origin at particle  $i$ , and so on (Fig. 2). In this regard, we make the changes of variables

$$\mathbf{R}_i = \mathbf{r}_M + \mathbf{p}, \quad \mathbf{R}_j = \mathbf{R}_i + \mathbf{R}_{ji}, \quad \text{etc.} \quad (6)$$

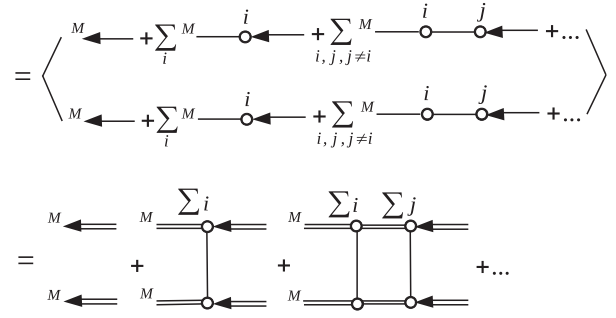


Fig. 3. Ladder approximation for the coherency dyadic.

The integration domain is the whole  $D_1$ . Therefore, for the direction  $\hat{\mathbf{p}}$ ,  $p$  ranges from zero at  $M$  to the corresponding value at the point  $C$  (where the straight line with the direction vector  $\hat{\mathbf{p}}$  crosses the lower plane boundary); for the direction  $\hat{\mathbf{R}}_{ji}$ ,  $R_{ji}$  ranges from zero at the origin at particle  $i$  to the corresponding value at the point  $C_i$  (where the straight line with the direction vector  $\hat{\mathbf{R}}_{ji}$  crosses the lower plane boundary), etc. Referring to Fig. 2, the coherency dyadic in the ladder approximation is given by

$$\begin{aligned} \bar{\mathbf{C}}(\mathbf{r}_M) = & \langle \mathbf{E}(\mathbf{r}_M) \otimes \mathbf{E}^*(\mathbf{r}_M) \rangle \\ = & \int_{\Omega^-} \delta(\hat{\mathbf{p}} + \hat{\mathbf{s}}) \bar{\mathbf{C}}_c(\mathbf{r}_M) d^2 \hat{\mathbf{p}} \\ & + n_0 \int_{\Omega^-} \left[ \int \bar{\mathbf{V}}(-\mathbf{p}, \hat{\mathbf{s}}) \cdot \bar{\mathbf{C}}_c(\mathbf{R}_i) \cdot \bar{\mathbf{V}}^\dagger(-\mathbf{p}, \hat{\mathbf{s}}) p^2 dp \right] d^2 \hat{\mathbf{p}} \\ & + n_0^2 \int_{\Omega^-} \left[ \int \bar{\mathbf{V}}(-\mathbf{p}, -\hat{\mathbf{R}}_{ji}) \cdot \bar{\mathbf{V}}(-\mathbf{R}_{ji}, \hat{\mathbf{s}}) \cdot \bar{\mathbf{C}}_c(\mathbf{R}_j) \right. \\ & \left. \cdot \bar{\mathbf{V}}^\dagger(-\mathbf{R}_{ji}, \hat{\mathbf{s}}) \cdot \bar{\mathbf{V}}^\dagger(-\mathbf{p}, -\hat{\mathbf{R}}_{ji}) p^2 R_{ji}^2 dR_{ji} d^2 \hat{\mathbf{R}}_{ji} dp \right] d^2 \hat{\mathbf{p}} + \dots, \end{aligned} \quad (7)$$

where  $\Omega^-$  is the lower unit half-sphere,  $\bar{\mathbf{C}}_c(\mathbf{r}_M) = \langle \mathbf{E}(\mathbf{r}_M) \rangle \otimes \langle \mathbf{E}^*(\mathbf{r}_M) \rangle$  is the coherent part of the coherency dyadic,  $\mathbf{E}_c(\mathbf{r}_M) = \langle \mathbf{E}(\mathbf{r}_M) \rangle$  is the coherent field, i.e.,

$$\begin{aligned} \mathbf{E}_c(\mathbf{r}_M) = & \overset{M}{\leftarrow} \\ = & \langle \overset{M}{\leftarrow} + \sum_i \overset{M}{\leftarrow} \overset{i}{\circ} \leftarrow + \sum_{i, j \neq i} \overset{M}{\leftarrow} \overset{i}{\circ} \overset{j}{\circ} \leftarrow + \dots \rangle, \end{aligned} \quad (8)$$

$\langle \cdot \rangle$  means the configuration average,  $\star$  and  $\dagger$  stand for the complex conjugate and the complex conjugate transpose (Hermitian transpose), respectively, and  $(\rho_{0i} = -\mathbf{p})$

$$\bar{\mathbf{V}}(\rho_{0i}, \hat{\mathbf{s}}) = \frac{\bar{\mathbf{t}}(\hat{\rho}_{0i}, \rho_{0i})}{\rho_{0i}} \cdot \bar{\mathbf{A}}(\hat{\rho}_{0i}, \hat{\mathbf{s}}), \quad (9)$$

$$\bar{\mathbf{t}}(\hat{\rho}_{0i}, \rho_{0i}) = \exp \left\{ \mathbf{j} \left[ k_1 \bar{\mathbf{I}} + \frac{2\pi}{k_1} n_0 \bar{\mathbf{A}}(\hat{\rho}_{0i}, \hat{\rho}_{0i}) \right] \rho_{0i} \right\}, \quad (10)$$

with  $\bar{\mathbf{I}}$  being the identity dyadic and  $n_0$  the number concentration of particles. A diagrammatic illustration of the coherency dyadic is shown in Fig. 3. The specific coherency dyadic at point  $M$  and in the upward direction  $\hat{\mathbf{q}} = -\hat{\mathbf{p}}$ ,  $\bar{\Sigma}(\mathbf{r}_M, -\hat{\mathbf{p}})$  is defined through the integral representation

$$\bar{\mathbf{C}}(\mathbf{r}_M) = \int_{\Omega^-} \bar{\Sigma}(\mathbf{r}_M, -\hat{\mathbf{p}}) d^2 \hat{\mathbf{p}}, \quad (11)$$

so that from Eq. (7), we have

$$\begin{aligned} \bar{\Sigma}(\mathbf{r}_M, -\hat{\mathbf{p}}) = & \delta(\hat{\mathbf{p}} + \hat{\mathbf{s}}) \bar{\mathbf{C}}_c(\mathbf{r}_M) \\ & + n_0 \int \bar{\mathbf{V}}(-\mathbf{p}, \hat{\mathbf{s}}) \cdot \bar{\mathbf{C}}_c(\mathbf{R}_i) \cdot \bar{\mathbf{V}}^\dagger(-\mathbf{p}, \hat{\mathbf{s}}) p^2 dp \end{aligned}$$

$$\begin{aligned}
& + n_0^2 \int \bar{\mathbf{V}}(-\mathbf{p}, -\hat{\mathbf{R}}_{ji}) \cdot \bar{\mathbf{V}}(-\mathbf{R}_{ji}, \hat{\mathbf{s}}) \cdot \bar{\mathbf{C}}_c(\mathbf{R}_j) \\
& \cdot \bar{\mathbf{V}}^\dagger(-\mathbf{R}_{ji}, \hat{\mathbf{s}}) \cdot \bar{\mathbf{V}}^\dagger(-\mathbf{p}, -\hat{\mathbf{R}}_{ji}) p^2 R_{ji}^2 dR_{ji} d^2 \hat{\mathbf{R}}_{ji} dp + \dots
\end{aligned} \quad (12)$$

It should be pointed out that under the Twersky approximation for the scattering system, the total field is evaluated at the point  $M$  on the average plane and not at the point  $M_S$  on the rough surface; therefore,  $\bar{\Sigma}(\mathbf{r}_M, -\hat{\mathbf{p}})$  is a deterministic quantity with respect to surface fluctuations.

**Step 2.** In the local coordinate system attached to  $M$ , the field scattered by particle  $i$  in its far-field region is a locally plane electromagnetic of amplitude  $\mathbf{E}_{0i}$  propagating in the direction  $\hat{\rho}_{0i}$ ,

$$\mathbf{E}_{\text{sct}i}^{(M)}(\boldsymbol{\rho}_0) = \mathbf{E}_{0i} e^{jk_1 \hat{\rho}_{0i} \cdot \boldsymbol{\rho}_0}, \quad (13)$$

with

$$\mathbf{E}_{0i} = \mathbf{E}_{\text{sct}i}(\mathbf{r}_M) = \frac{e^{jk_1 \rho_{0i}}}{\rho_{0i}} \mathbf{E}_{\text{sct}i}^\infty(\hat{\rho}_{0i}), \quad (14)$$

being the scattered field at  $M$ . Similarly, the incident field is a plane electromagnetic wave of amplitude  $\mathbf{E}_0(\mathbf{r}_M)$  propagating in the direction  $\hat{\mathbf{s}}$ ,

$$\mathbf{E}_0^{(M)}(\boldsymbol{\rho}_0) = \mathbf{E}_0(\mathbf{r}_M) e^{jk_1 \hat{\mathbf{s}} \cdot \boldsymbol{\rho}_0}. \quad (15)$$

In general, for an incident plane electromagnetic wave  $\mathbf{E}_0(\mathbf{r})$  as in Eq. (1), the field reflected by a rough surface is given by

$$\mathbf{E}_R(\boldsymbol{\rho}) = \frac{e^{jk_1 \rho}}{\rho} \bar{\mathbf{A}}_{\text{SR}}(\hat{\mathbf{q}}_R, \hat{\mathbf{s}}) \cdot \mathbf{E}_0(\mathbf{r}_M), \quad (16)$$

where  $\bar{\mathbf{A}}_{\text{SR}}$  is the local scattering reflection dyadic of the rough surface. We assume that each elementary element of the rough interface scatters a plane electromagnetic wave as if the rest of the surface did not exist. Taking into account that the incident field at  $M$  is a superposition of the incident plane electromagnetic wave and of local plane electromagnetic waves coming from all the particles, we deduce that the reflected field at  $P$  is

$$\mathbf{E}_R(\boldsymbol{\rho}) = \frac{e^{jk_1 \rho}}{\rho} \mathbf{E}_R^\infty(\hat{\mathbf{q}}_R), \quad (17)$$

where the far-field pattern  $\mathbf{E}_R^\infty$  is

$$\mathbf{E}_R^\infty(\hat{\mathbf{q}}_R) = \bar{\mathbf{A}}_{\text{SR}}(\hat{\mathbf{q}}_R, \hat{\mathbf{s}}) \cdot \mathbf{E}_0(\mathbf{r}_M) + \sum_i \bar{\mathbf{A}}_{\text{SR}}(\hat{\mathbf{q}}_R, \hat{\rho}_{0i}) \cdot \mathbf{E}_{0i}. \quad (18)$$

By means of the Twersky approximation, an order-of-scattering expansion for  $\mathbf{E}_R^\infty$  reads as

$$\begin{aligned}
\mathbf{E}_R^\infty(\hat{\mathbf{q}}_R) & = \bar{\mathbf{A}}_{\text{SR}}(\hat{\mathbf{q}}_R, \hat{\mathbf{s}}) \cdot \mathbf{E}_0(\mathbf{r}_M) \\
& + \sum_i \bar{\mathbf{A}}_{\text{SR}}(\hat{\mathbf{q}}_R, \hat{\rho}_{0i}) \cdot \frac{e^{jk_1 \rho_{0i}}}{\rho_{0i}} \bar{\mathbf{A}}(\hat{\rho}_{0i}, \hat{\mathbf{s}}) \cdot \mathbf{E}_0(\mathbf{R}_i) \\
& + \sum_{i,j,j \neq i} \bar{\mathbf{A}}_{\text{SR}}(\hat{\mathbf{q}}_R, \hat{\rho}_{0i}) \cdot \frac{e^{jk_1 \rho_{0i}}}{\rho_{0i}} \bar{\mathbf{A}}(\hat{\rho}_{0i}, \hat{\mathbf{R}}_{ij}) \\
& \cdot \frac{e^{jk_1 R_{ij}}}{R_{ij}} \bar{\mathbf{A}}(\hat{\mathbf{R}}_{ij}, \hat{\mathbf{s}}) \cdot \mathbf{E}_0(\mathbf{R}_j) + \dots,
\end{aligned} \quad (19)$$

or in diagrammatic representation,

$$\mathbf{E}_R^\infty = \diamond \leftarrow + \sum_i \diamond \leftarrow \overset{i}{\leftarrow} + \sum_{i,j,j \neq i} \diamond \leftarrow \overset{i}{\leftarrow} \overset{j}{\leftarrow} + \dots, \quad (20)$$

where, the symbol  $\diamond$  means multiplying a field at  $M$  by the scattering reflection dyadic  $\bar{\mathbf{A}}_{\text{SR}}$ . From Eq. (8), it is apparent that the

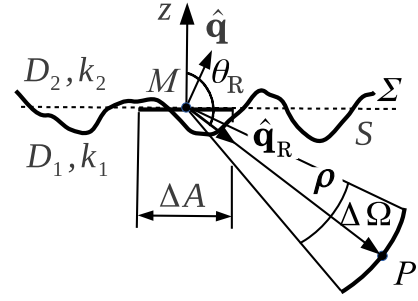


Fig. 4. Incidence and reflection directions  $\hat{\mathbf{q}}$  and  $\hat{\mathbf{q}}_R$ , respectively, and the area of the illuminated surface  $\Delta A$ .

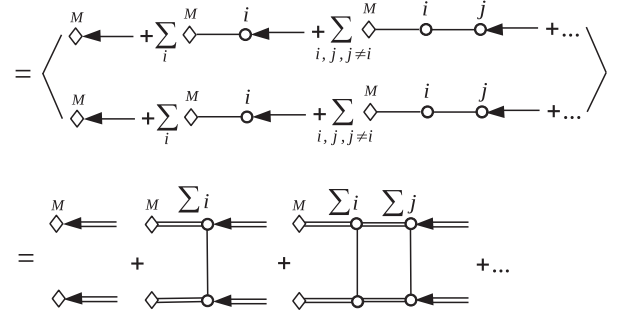


Fig. 5. Ladder approximation of  $(\mathbf{E}_R^\infty \otimes \mathbf{E}_R^{\infty*})$ .

configuration average of  $\mathbf{E}_R^\infty$  is

$$\begin{aligned}
\langle \mathbf{E}_R^\infty \rangle & = \langle \diamond \leftarrow + \sum_i \diamond \leftarrow \overset{i}{\leftarrow} + \sum_{i,j,j \neq i} \diamond \leftarrow \overset{i}{\leftarrow} \overset{j}{\leftarrow} + \dots \rangle \\
& = \diamond \leftarrow \Leftarrow,
\end{aligned} \quad (21)$$

that is,

$$\langle \mathbf{E}_R^\infty(\hat{\mathbf{q}}_R) \rangle = \bar{\mathbf{A}}_{\text{SR}}(\hat{\mathbf{q}}_R, \hat{\mathbf{s}}) \cdot \mathbf{E}_c(\mathbf{r}_M). \quad (22)$$

We define the (elementary) reflection coherency dyadic at  $M$  in an elementary solid angle  $\Delta\Omega$  around  $\hat{\mathbf{q}}_R$  by (cf. Eq. (17))

$$\Delta \bar{\mathbf{C}}(\mathbf{r}_M, \hat{\mathbf{q}}_R) := \bar{\Sigma}(\mathbf{r}_M, \hat{\mathbf{q}}_R) \Delta\Omega = \frac{1}{\rho^2} (\mathbf{E}_R^\infty(\hat{\mathbf{q}}_R) \otimes \mathbf{E}_R^{\infty*}(\hat{\mathbf{q}}_R)), \quad (23)$$

where  $\bar{\Sigma}(\mathbf{r}_M, \hat{\mathbf{q}}_R)$  is the specific reflection coherency dyadic. Here, we do not use a special notation for the (specific) reflection coherency dyadic; the argument  $\hat{\mathbf{q}}_R$ , indicating a downward reflection direction, specifies the type of the (specific) coherency dyadic. Using

$$\Delta\Omega = \frac{\Delta A}{\rho^2} |\cos \theta_R|, \quad (24)$$

where  $\Delta A$  is the (elementary) area of the illuminated surface (Fig. 4), we find that the specific reflection coherency dyadic can be written as

$$\bar{\Sigma}(\mathbf{r}_M, \hat{\mathbf{q}}_R) = \frac{1}{\Delta A |\cos \theta_R|} (\mathbf{E}_R^\infty(\hat{\mathbf{q}}_R) \otimes \mathbf{E}_R^{\infty*}(\hat{\mathbf{q}}_R)). \quad (25)$$

To compute  $(\mathbf{E}_R^\infty \otimes \mathbf{E}_R^{\infty*})$ , appearing on the right-hand side of Eq. (25), we employ the ladder approximation, illustrated diagrammatically in Fig. 5. By means of Eq. (12), we find

$$\begin{aligned}
\bar{\Sigma}(\mathbf{r}_M, \hat{\mathbf{q}}_R) & = \frac{1}{\Delta A |\cos \theta_R|} \left\{ \int_{\Omega^-} \delta(\hat{\mathbf{p}} + \hat{\mathbf{s}}) \bar{\mathbf{A}}_{\text{SR}}(\hat{\mathbf{q}}_R, -\hat{\mathbf{p}}) \cdot \bar{\mathbf{C}}_c(\mathbf{r}_M) \right. \\
& \cdot \bar{\mathbf{A}}_{\text{SR}}^\dagger(\hat{\mathbf{q}}_R, -\hat{\mathbf{p}}) d^2 \hat{\mathbf{p}} \\
& \left. + n_0 \int_{\Omega^-} \left[ \int \bar{\mathbf{A}}_{\text{SR}}(\hat{\mathbf{q}}_R, -\hat{\mathbf{p}}) \cdot \bar{\mathbf{V}}(-\mathbf{p}, \hat{\mathbf{s}}) \cdot \bar{\mathbf{C}}_c(\mathbf{R}_i) \right. \right.
\end{aligned}$$

$$\begin{aligned}
& \cdot \bar{\mathbf{V}}^\dagger(-\mathbf{p}, \hat{\mathbf{s}}) \cdot \bar{\mathbf{A}}_{\text{SR}}^\dagger(\hat{\mathbf{q}}_{\text{R}}, -\hat{\mathbf{p}}) p^2 dp \Big] d^2 \hat{\mathbf{p}} \\
& + n_0^2 \int_{\Omega^-} \left[ \int \bar{\mathbf{A}}_{\text{SR}}(\hat{\mathbf{q}}_{\text{R}}, -\hat{\mathbf{p}}) \cdot \bar{\mathbf{V}}(-\mathbf{p}, -\hat{\mathbf{R}}_{ji}) \cdot \bar{\mathbf{V}}(-\mathbf{R}_{ji}, \hat{\mathbf{s}}) \right. \\
& \cdot \bar{\mathbf{C}}_{\text{c}}(\mathbf{R}_{ji}) \cdot \bar{\mathbf{V}}^\dagger(-\mathbf{R}_{ji}, \hat{\mathbf{s}}) \cdot \bar{\mathbf{V}}^\dagger(-\mathbf{p}, -\hat{\mathbf{R}}_{ji}) \cdot \bar{\mathbf{A}}_{\text{SR}}^\dagger(\hat{\mathbf{q}}_{\text{R}}, -\hat{\mathbf{p}}) \\
& \times p^2 R_{ji}^2 d\mathbf{R}_{ji} d^2 \hat{\mathbf{R}}_{ji} dp \Big] d^2 \hat{\mathbf{p}} + \dots \Big\} \\
& = \frac{1}{\Delta A |\cos \theta_{\text{R}}|} \int_{\Omega^+} \bar{\mathbf{A}}_{\text{SR}}(\hat{\mathbf{q}}_{\text{R}}, \hat{\mathbf{q}}) \cdot \bar{\Sigma}(\mathbf{r}_{\text{M}}, \hat{\mathbf{q}}) \cdot \bar{\mathbf{A}}_{\text{SR}}^\dagger(\hat{\mathbf{q}}_{\text{R}}, \hat{\mathbf{q}}) d^2 \hat{\mathbf{q}}, \quad (26)
\end{aligned}$$

where  $\Omega^+$  is the upper unit half-sphere. Finally, taking the average over surface fluctuations, applying the dyadic identity  $(\bar{\mathbf{A}} \otimes \bar{\mathbf{B}}) \cdot \bar{\mathbf{C}} = \bar{\mathbf{A}} \cdot \bar{\mathbf{C}} \cdot \bar{\mathbf{B}}^T$ , where  $\bar{\mathbf{A}}^T$  is the transpose of  $\bar{\mathbf{A}}$ , and using  $\langle \bar{\Sigma}(\mathbf{r}_{\text{M}}, \hat{\mathbf{q}}) \rangle_S = \bar{\Sigma}(\mathbf{r}_{\text{M}}, \hat{\mathbf{q}})$  (because  $\bar{\Sigma}(\mathbf{r}_{\text{M}}, \hat{\mathbf{q}})$  is deterministic), we obtain

$$\begin{aligned}
\langle \bar{\Sigma}(\mathbf{r}_{\text{M}}, \hat{\mathbf{q}}_{\text{R}}) \rangle_S & = \frac{1}{\Delta A |\cos \theta_{\text{R}}|} \int_{\Omega^+} \langle \bar{\mathbf{A}}_{\text{SR}}(\hat{\mathbf{q}}_{\text{R}}, \hat{\mathbf{q}}) \otimes \bar{\mathbf{A}}_{\text{SR}}^*(\hat{\mathbf{q}}_{\text{R}}, \hat{\mathbf{q}}) \rangle_S \\
& \cdot \langle \bar{\Sigma}(\mathbf{r}_{\text{M}}, \hat{\mathbf{q}}) \rangle_S d^2 \hat{\mathbf{q}}, \quad (27)
\end{aligned}$$

where  $\langle \cdot \rangle_S$  means the average over surface fluctuations.

To compute  $\langle \bar{\mathbf{A}}_{\text{SR}} \otimes \bar{\mathbf{A}}_{\text{SR}}^* \rangle_S$ , any asymptotic method available in rough surface scattering theory can be used [10,11,19,20]. In the Kirchhoff approach and the geometrical optics approximation, the scattering reflection dyadic is given by [11]

$$\begin{aligned}
\bar{\mathbf{A}}_{\text{SR}}(\hat{\mathbf{q}}_{\text{R}}, \hat{\mathbf{q}}) & = -2\pi j k_1 |\cos \theta_{\text{R}}| \bar{\mathbf{R}}_{21}(k_1 \hat{\mathbf{q}}_{\text{R}\perp}, k_1 \hat{\mathbf{q}}_{\perp}) \\
& = \frac{j k_1}{4\pi} c_{\text{R}}(\hat{\mathbf{q}}_{\text{R}}, \hat{\mathbf{q}}) I_{\text{R}}^h(\hat{\mathbf{q}}_{\text{R}}, \hat{\mathbf{q}}) \bar{\mathbf{r}}_{21}(\hat{\mathbf{q}}_{\text{R}}, \hat{\mathbf{q}}), \quad (28)
\end{aligned}$$

where  $\bar{\mathbf{R}}_{21}$  is the reflection dyadic,  $\hat{\mathbf{q}}_{\text{R}} = \hat{\mathbf{q}}_{\text{R}\perp} + (\hat{\mathbf{q}}_{\text{R}} \cdot \hat{\mathbf{z}}) \hat{\mathbf{z}}$ ,

$$c_{\text{R}}(\hat{\mathbf{q}}_{\text{R}}, \hat{\mathbf{q}}) = \frac{|\hat{\mathbf{q}} - \hat{\mathbf{q}}_{\text{R}}|^2}{|\hat{\mathbf{q}} \times \hat{\mathbf{q}}_{\text{R}}| |\hat{\mathbf{q}} - \hat{\mathbf{q}}_{\text{R}}| \cdot \hat{\mathbf{z}}}, \quad (29)$$

$$I_{\text{R}}^h(\hat{\mathbf{q}}_{\text{R}}, \hat{\mathbf{q}}) = \int_{\Delta A} e^{j k_1 (\hat{\mathbf{q}} - \hat{\mathbf{q}}_{\text{R}}) \cdot \boldsymbol{\rho}_0} d^2 \boldsymbol{\rho}_{0\perp}, \quad (30)$$

$\boldsymbol{\rho}_0 = \boldsymbol{\rho}_{0\perp} + h(\boldsymbol{\rho}_{0\perp}) \hat{\mathbf{z}}$ , and  $\bar{\mathbf{r}}_{21}$  is the two-dimensional dyadic

$$\bar{\mathbf{r}}_{21}(\hat{\mathbf{q}}_{\text{R}}, \hat{\mathbf{q}}) = \sum_{\eta, \mu = \varphi, \theta} r_{\eta\mu}(\hat{\mathbf{q}}_{\text{R}}, \hat{\mathbf{q}}) \hat{\boldsymbol{\eta}}(\hat{\mathbf{q}}_{\text{R}}) \otimes \hat{\boldsymbol{\mu}}(\hat{\mathbf{q}}) \quad (31)$$

with entries

$$r_{\varphi\varphi}(\hat{\mathbf{q}}_{\text{R}}, \hat{\mathbf{q}}) = r_{\parallel}[\hat{\boldsymbol{\varphi}}(\hat{\mathbf{q}}) \cdot \hat{\mathbf{q}}_{\text{R}}][\hat{\boldsymbol{\varphi}}(\hat{\mathbf{q}}_{\text{R}}) \cdot \hat{\mathbf{q}}] + r_{\perp}[\hat{\boldsymbol{\theta}}(\hat{\mathbf{q}}) \cdot \hat{\mathbf{q}}_{\text{R}}][\hat{\boldsymbol{\theta}}(\hat{\mathbf{q}}_{\text{R}}) \cdot \hat{\mathbf{q}}], \quad (32)$$

$$r_{\varphi\theta}(\hat{\mathbf{q}}_{\text{R}}, \hat{\mathbf{q}}) = r_{\parallel}[\hat{\boldsymbol{\theta}}(\hat{\mathbf{q}}) \cdot \hat{\mathbf{q}}_{\text{R}}][\hat{\boldsymbol{\varphi}}(\hat{\mathbf{q}}_{\text{R}}) \cdot \hat{\mathbf{q}}] - r_{\perp}[\hat{\boldsymbol{\varphi}}(\hat{\mathbf{q}}) \cdot \hat{\mathbf{q}}_{\text{R}}][\hat{\boldsymbol{\theta}}(\hat{\mathbf{q}}_{\text{R}}) \cdot \hat{\mathbf{q}}], \quad (33)$$

$$r_{\theta\varphi}(\hat{\mathbf{q}}_{\text{R}}, \hat{\mathbf{q}}) = r_{\parallel}[\hat{\boldsymbol{\varphi}}(\hat{\mathbf{q}}) \cdot \hat{\mathbf{q}}_{\text{R}}][\hat{\boldsymbol{\theta}}(\hat{\mathbf{q}}_{\text{R}}) \cdot \hat{\mathbf{q}}] - r_{\perp}[\hat{\boldsymbol{\theta}}(\hat{\mathbf{q}}) \cdot \hat{\mathbf{q}}_{\text{R}}][\hat{\boldsymbol{\varphi}}(\hat{\mathbf{q}}_{\text{R}}) \cdot \hat{\mathbf{q}}], \quad (34)$$

$$r_{\theta\theta}(\hat{\mathbf{q}}_{\text{R}}, \hat{\mathbf{q}}) = r_{\parallel}[\hat{\boldsymbol{\theta}}(\hat{\mathbf{q}}) \cdot \hat{\mathbf{q}}_{\text{R}}][\hat{\boldsymbol{\theta}}(\hat{\mathbf{q}}_{\text{R}}) \cdot \hat{\mathbf{q}}] + r_{\perp}[\hat{\boldsymbol{\varphi}}(\hat{\mathbf{q}}) \cdot \hat{\mathbf{q}}_{\text{R}}][\hat{\boldsymbol{\varphi}}(\hat{\mathbf{q}}_{\text{R}}) \cdot \hat{\mathbf{q}}]. \quad (35)$$

The lower subscripts in the notations of the dyadics  $\bar{\mathbf{R}}_{21}$  and  $\bar{\mathbf{r}}_{21}$  indicate that the incident wave propagates from medium  $D_1$  to medium  $D_2$ . In Eqs. (32)–(35),

$$r_{\perp} = r_{\perp}(\theta_{\text{L}0}) = \frac{\cos \theta_{\text{L}0} - \sqrt{m^2 - 1 + \cos^2 \theta_{\text{L}0}}}{\cos \theta_{\text{L}0} + \sqrt{m^2 - 1 + \cos^2 \theta_{\text{L}0}}}, \quad (36)$$

$$r_{\parallel} = r_{\parallel}(\theta_{\text{L}0}) = \frac{m^2 \cos \theta_{\text{L}0} - \sqrt{m^2 - 1 + \cos^2 \theta_{\text{L}0}}}{m^2 \cos \theta_{\text{L}0} + \sqrt{m^2 - 1 + \cos^2 \theta_{\text{L}0}}}, \quad (37)$$

are the Fresnel reflection coefficients,  $\cos \theta_{\text{L}0} = -\hat{\mathbf{n}}_0 \cdot \hat{\mathbf{q}}$  is the cosine of the local incident angle  $\theta_{\text{L}0}$ , and

$$\hat{\mathbf{n}}_0 = \frac{\hat{\mathbf{q}}_{\text{R}} - \hat{\mathbf{q}}}{|\hat{\mathbf{q}}_{\text{R}} - \hat{\mathbf{q}}|} \quad (38)$$

the surface normal unit vector at  $M_S$  pointing in  $D_1$ . Eq. (38) reveals that the incident and reflected wave directions form a specular reflection. From Eq. (28) it is apparent that the computation of  $\langle \bar{\mathbf{A}}_{\text{SR}}(\hat{\mathbf{q}}_{\text{R}}, \hat{\mathbf{q}}) \otimes \bar{\mathbf{A}}_{\text{SR}}^*(\hat{\mathbf{q}}_{\text{R}}, \hat{\mathbf{q}}) \rangle_S$  reduces to the computation of  $\langle I_{\text{R}}^h(\hat{\mathbf{q}}_{\text{R}}, \hat{\mathbf{q}}) I_{\text{R}}^{h*}(\hat{\mathbf{q}}_{\text{R}}, \hat{\mathbf{q}}) \rangle_S$ . For doing this, the integral

$$\begin{aligned}
I_{\text{R}}^h(\hat{\mathbf{q}}_{\text{R}}, \hat{\mathbf{q}}) I_{\text{R}}^{h*}(\hat{\mathbf{q}}_{\text{R}}, \hat{\mathbf{q}}) & = \int_{\Delta A} e^{j \mathbf{t}_{\perp} \cdot (\boldsymbol{\rho}_{0\perp} - \boldsymbol{\rho}'_{0\perp})} \\
& \times e^{j t_z [h(\boldsymbol{\rho}_{0\perp}) - h(\boldsymbol{\rho}'_{0\perp})]} d^2 \boldsymbol{\rho}'_{0\perp} d^2 \boldsymbol{\rho}_{0\perp}, \quad (39)
\end{aligned}$$

with

$$\mathbf{t} = k_1 (\hat{\mathbf{q}} - \hat{\mathbf{q}}_{\text{R}}) = t_{\perp} + t_z \hat{\mathbf{z}}, \quad (40)$$

$$\mathbf{t}_{\perp} = t_x \hat{\mathbf{x}} + t_y \hat{\mathbf{y}}, \quad (41)$$

$$t_z = \mathbf{t} \cdot \hat{\mathbf{z}} = k_1 (\hat{\mathbf{q}} - \hat{\mathbf{q}}_{\text{R}}) \cdot \hat{\mathbf{z}}, \quad (42)$$

is first computed by the asymptotic method, and then the average over surface fluctuations is taken; the result is

$$\langle I_{\text{R}}^h(\hat{\mathbf{q}}_{\text{R}}, \hat{\mathbf{q}}) I_{\text{R}}^{h*}(\hat{\mathbf{q}}_{\text{R}}, \hat{\mathbf{q}}) \rangle_S = \frac{(2\pi)^2 \Delta A}{t_z^2} p\left(-\frac{t_x}{t_z}, -\frac{t_y}{t_z}\right), \quad (43)$$

where  $p(\alpha, \beta)$  is the probability density function for the slopes of the surface. For the Gaussian probability density function

$$p(\alpha, \beta) = \frac{1}{2\pi s^2} \exp\left(-\frac{\alpha^2 + \beta^2}{2s^2}\right), \quad (44)$$

where  $s^2$  is the mean square surface slope, we end up with

$$\langle I_{\text{R}}^h(\hat{\mathbf{q}}_{\text{R}}, \hat{\mathbf{q}}) I_{\text{R}}^{h*}(\hat{\mathbf{q}}_{\text{R}}, \hat{\mathbf{q}}) \rangle_S = \frac{2\pi \Delta A}{t_z^2 s^2} \exp\left(-\frac{t_x^2 + t_y^2}{2t_z^2 s^2}\right). \quad (45)$$

Taking account of Eq. (45), we then obtain

$$\begin{aligned}
\langle \bar{\Sigma}(\mathbf{r}_{\text{M}}, \hat{\mathbf{q}}_{\text{R}}) \rangle_S & = \frac{1}{8\pi |\cos \theta_{\text{R}}|} \int_{\Omega^+} \frac{|\hat{\mathbf{q}} - \hat{\mathbf{q}}_{\text{R}}|^4}{|\hat{\mathbf{q}} \times \hat{\mathbf{q}}_{\text{R}}|^4 |(\hat{\mathbf{q}} - \hat{\mathbf{q}}_{\text{R}}) \cdot \hat{\mathbf{z}}|^4 s^2} \\
& \times \exp\left(-\frac{t_x^2 + t_y^2}{2t_z^2 s^2}\right) \bar{\mathbf{r}}_{21}(\hat{\mathbf{q}}_{\text{R}}, \hat{\mathbf{q}}) \cdot \langle \bar{\Sigma}(\mathbf{r}_{\text{M}}, \hat{\mathbf{q}}) \rangle_S \\
& \cdot \bar{\mathbf{r}}_{21}^\dagger(\hat{\mathbf{q}}_{\text{R}}, \hat{\mathbf{q}}) d^2 \hat{\mathbf{q}}. \quad (46)
\end{aligned}$$

For a plane surface, the scattering reflection dyadic is

$$\bar{\mathbf{A}}_{\text{SR}}(\hat{\mathbf{q}}_{\text{R}}, \hat{\mathbf{q}}) = -2\pi j k_1 |\cos \theta_{\text{R}}| \delta(\mathbf{q}_{\perp} - \mathbf{q}_{\text{R}\perp}) \bar{\mathbf{R}}_{21}(\mathbf{q}_{\text{R}\perp}, \mathbf{q}_{\perp}), \quad (47)$$

where  $\mathbf{q}_{\perp} = k_1 \hat{\mathbf{q}}_{\perp}$  and  $\mathbf{q}_{\text{R}\perp} = k_1 \hat{\mathbf{q}}_{\text{R}\perp}$ , while the reflection dyadic  $\bar{\mathbf{R}}_{21}$  is

$$\bar{\mathbf{R}}_{21}(\mathbf{q}_{\text{R}\perp}, \mathbf{q}_{\perp}) = r_{\parallel} \hat{\boldsymbol{\theta}}(\hat{\mathbf{q}}_{\text{R}}) \otimes \hat{\boldsymbol{\theta}}(\hat{\mathbf{q}}) + r_{\perp} \hat{\boldsymbol{\varphi}}(\hat{\mathbf{q}}_{\text{R}}) \otimes \hat{\boldsymbol{\varphi}}(\hat{\mathbf{q}}). \quad (48)$$

If the illuminated area is infinite, we have then to replace  $\Delta A$  in Eq. (26) by  $(2\pi)^2 \delta(\mathbf{q}_{\perp} - \mathbf{q}_{\text{R}\perp})$ , so that inserting Eq. (47) in (26) and taking account of

$$d^2 \hat{\mathbf{q}} = \frac{1}{k_1^2 \cos \theta} d^2 \mathbf{q}_{\perp}, \quad (49)$$

we get the boundary condition for the specific coherency dyadic

$$\bar{\Sigma}(\mathbf{r}_{\text{M}}, \hat{\mathbf{q}}_{\text{R}}) = \bar{\mathbf{R}}_{21}(\mathbf{q}_{\text{R}\perp}, \mathbf{q}_{\perp}) \cdot \bar{\Sigma}(\mathbf{r}_{\text{M}}, \hat{\mathbf{q}}) \cdot \bar{\mathbf{R}}_{21}^\dagger(\mathbf{q}_{\text{R}\perp}, \mathbf{q}_{\perp}), \quad (50)$$

where  $(\hat{\mathbf{q}}, \hat{\mathbf{q}}_{\text{R}}, \hat{\mathbf{n}}_0 = -\hat{\mathbf{z}})$  is a system of specular reflection directions.

## 2.2. Transmission

To establish the boundary condition for the transmitted field we proceed analogously. For the upward transmission direction  $\hat{\mathbf{q}}_{\text{T}} = \hat{\mathbf{q}}_{\text{T}}(\theta_{\text{T}}, \varphi_{\text{T}})$  characterized by the polar and azimuthal angles  $\theta_{\text{T}}$  and  $\varphi_{\text{T}}$ , respectively, with  $\theta_{\text{T}} < \pi/2$  (Fig. 6), we define the (elementary)



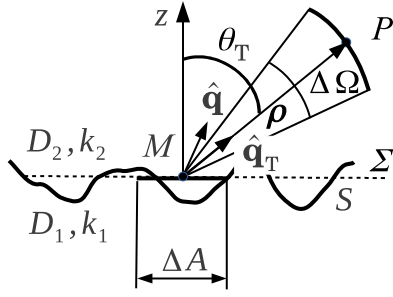


**Fig. 6.** Incidence and transmission directions  $\hat{\mathbf{q}}$  and  $\hat{\mathbf{q}}_T$ , respectively, and the area of the illuminated surface  $\Delta A$ .

transmission coherency dyadic at  $M$  in an elementary solid angle  $\Delta\Omega$  around  $\hat{\mathbf{q}}_T$  by

$$\Delta\bar{\mathbf{C}}(\mathbf{r}_M, \hat{\mathbf{q}}_T) := \bar{\Sigma}(\mathbf{r}_M, \hat{\mathbf{q}}_T)\Delta\Omega = \frac{1}{\rho^2} \langle \mathbf{E}_T^\infty(\hat{\mathbf{q}}_T) \otimes \mathbf{E}_T^{\infty*}(\hat{\mathbf{q}}_T) \rangle, \quad (51)$$

where  $\mathbf{E}_T^\infty$  is the far-field pattern of the transmitted field and  $\bar{\Sigma}(\mathbf{r}_M, \hat{\mathbf{q}}_T)$  the specific transmission coherency dyadic. The final result is

$$\langle \bar{\Sigma}(\mathbf{r}_M, \hat{\mathbf{q}}_T) \rangle_S = \frac{1}{\Delta A \cos \theta_T} \int_{\Omega^+} \langle \bar{\mathbf{A}}_{ST}(\hat{\mathbf{q}}_T, \hat{\mathbf{q}}) \otimes \bar{\mathbf{A}}_{ST}^*(\hat{\mathbf{q}}_T, \hat{\mathbf{q}}) \rangle_S \cdot \langle \bar{\Sigma}(\mathbf{r}_M, \hat{\mathbf{q}}) \rangle_S d^2\hat{\mathbf{q}}, \quad (52)$$

where  $\bar{\mathbf{A}}_{ST}$  is the scattering transmission dyadic of the rough surface.

In the Kirchhoff approach and the geometrical optics approximation, the scattering transmission dyadic is given by [11]

$$\begin{aligned} \bar{\mathbf{A}}_{ST}(\hat{\mathbf{q}}_T, \hat{\mathbf{q}}) &= -2\pi j k_2 \cos \theta_T \bar{\mathbf{T}}_{21}(k_2 \hat{\mathbf{q}}_{T\perp}, k_1 \hat{\mathbf{q}}_{\perp}) \\ &= -\frac{j k_2}{4\pi} c_T(\hat{\mathbf{q}}_T, \hat{\mathbf{q}}) I_T^h(\hat{\mathbf{q}}_T, \hat{\mathbf{q}}) \bar{\mathbf{T}}_{21}(\hat{\mathbf{q}}_T, \hat{\mathbf{q}}), \end{aligned} \quad (53)$$

where  $\bar{\mathbf{T}}_{21}$  is the transmission dyadic,

$$c_T(\hat{\mathbf{q}}_T, \hat{\mathbf{q}}) = \frac{2 |\hat{\mathbf{n}}_0 \cdot \hat{\mathbf{q}}_T| |\hat{\mathbf{q}} - m\hat{\mathbf{q}}_T|}{|\hat{\mathbf{q}} \times \hat{\mathbf{q}}_T|^2 |(\hat{\mathbf{q}} - m\hat{\mathbf{q}}_T) \cdot \hat{\mathbf{z}}|}, \quad (54)$$

$$I_T^h(\hat{\mathbf{q}}_T, \hat{\mathbf{q}}) = \int_{\Delta A} e^{j(k_1 \hat{\mathbf{q}} - k_2 \hat{\mathbf{q}}_T) \cdot \rho_0} d^2\rho_{0\perp}, \quad (55)$$

and

$$\hat{\mathbf{n}}_0 = \frac{k_1 \hat{\mathbf{q}} - k_2 \hat{\mathbf{q}}_T}{|k_1 \hat{\mathbf{q}} - k_2 \hat{\mathbf{q}}_T|} = \frac{\hat{\mathbf{q}} - m\hat{\mathbf{q}}_T}{|\hat{\mathbf{q}} - m\hat{\mathbf{q}}_T|} \quad (56)$$

is the surface normal unit vector at  $M_S$  pointing in  $D_1$ . The relation (56) is an equivalent statement of Snell's law; thus, the incident and transmitted wave directions form a specular transmission. The entries of the two-dimensional dyadic

$$\bar{\mathbf{T}}_{21}(\hat{\mathbf{q}}_T, \hat{\mathbf{q}}) = \sum_{\eta, \mu = \varphi, \theta} t_{\eta\mu}(\hat{\mathbf{q}}_T, \hat{\mathbf{q}}) \hat{\boldsymbol{\eta}}(\hat{\mathbf{q}}_T) \otimes \hat{\boldsymbol{\mu}}(\hat{\mathbf{q}}) \quad (57)$$

are given by Eqs. (32)–(35) with  $\hat{\mathbf{q}}_T$  in place of  $\hat{\mathbf{q}}_R$ , and with the Fresnel transmission coefficients ( $\cos \theta_{L0} = -\hat{\mathbf{n}}_0 \cdot \hat{\mathbf{q}}$ )

$$t_{\perp}(\theta_{L0}) = \frac{2 \cos \theta_{L0}}{\cos \theta_{L0} + \sqrt{m^2 - 1 + \cos^2 \theta_{L0}}} = 1 + r_{\perp}(\theta_{L0}) \quad (58)$$

$$t_{\parallel}(\theta_{L0}) = \frac{2m \cos \theta_{L0}}{m^2 \cos \theta_{L0} + \sqrt{m^2 - 1 + \cos^2 \theta_{L0}}} = \frac{1}{m} [1 + r_{\parallel}(\theta_{L0})] \quad (59)$$

in place of the Fresnel reflection coefficients  $r_{\perp}(\theta_{L0})$  and  $r_{\parallel}(\theta_{L0})$ , respectively. By using

$$\langle I_T^h(\hat{\mathbf{q}}_T, \hat{\mathbf{q}}) I_T^{h*}(\hat{\mathbf{q}}_T, \hat{\mathbf{q}}) \rangle_S = \frac{2\pi \Delta A}{t_z^2 s^2} \exp\left(-\frac{t_x^2 + t_y^2}{2t_z^2 s^2}\right), \quad (60)$$

$$\mathbf{t} = k_1 \hat{\mathbf{q}} - k_2 \hat{\mathbf{q}}_T = k_1 (\hat{\mathbf{q}} - m\hat{\mathbf{q}}_T) = \mathbf{t}_{\perp} + t_z \hat{\mathbf{z}}, \quad (61)$$

$$\mathbf{t}_{\perp} = t_x \hat{\mathbf{x}} + t_y \hat{\mathbf{y}}, \quad (62)$$

$$t_z = \mathbf{t} \cdot \hat{\mathbf{z}} = k_1 (\hat{\mathbf{q}} - m\hat{\mathbf{q}}_T) \cdot \hat{\mathbf{z}}, \quad (63)$$

we obtain the boundary condition for the specific coherency dyadic

$$\begin{aligned} \langle \bar{\Sigma}(\mathbf{r}_M, \hat{\mathbf{q}}_T) \rangle_S &= \frac{m^2}{2\pi \cos \theta_T} \int_{\Omega^+} \frac{|\hat{\mathbf{q}} - m\hat{\mathbf{q}}_T \cdot \hat{\mathbf{q}}|^2}{|\hat{\mathbf{q}} \times \hat{\mathbf{q}}_T|^4 |(\hat{\mathbf{q}} - m\hat{\mathbf{q}}_T) \cdot \hat{\mathbf{z}}|^4 s^2} \\ &\times \exp\left(-\frac{t_x^2 + t_y^2}{2t_z^2 s^2}\right) \bar{\mathbf{T}}_{21}(\hat{\mathbf{q}}_T, \hat{\mathbf{q}}) \cdot \langle \bar{\Sigma}(\mathbf{r}_M, \hat{\mathbf{q}}) \rangle_S \\ &\cdot \bar{\mathbf{T}}_{21}^\dagger(\hat{\mathbf{q}}_T, \hat{\mathbf{q}}) d^2\hat{\mathbf{q}}. \end{aligned} \quad (64)$$

At this stage of our presentation, a brief remark is in order. Strictly speaking, the geometrical optics approximation applies if the domain  $D_2$  is non-absorbing, since otherwise, at the stationary point, the surface slopes are complex quantities. However, as in the Snell law, when the transmission angle can be complex, we may admit, by an analytic continuation procedure, that the surface slopes can be also complex. In this case, the above results are valid for an absorbing domain  $D_2$ .

For a plane surface, the scattering transmission dyadic is

$$\bar{\mathbf{A}}_{ST}(\hat{\mathbf{q}}_T, \hat{\mathbf{q}}) = -2\pi j k_2 \cos \theta_T \delta(\mathbf{q}_{\perp} - \mathbf{q}_{T\perp}) \bar{\mathbf{T}}_{21}(k_2 \hat{\mathbf{q}}_{T\perp}, k_1 \hat{\mathbf{q}}_{\perp}), \quad (65)$$

where, for  $\mathbf{q}_{\perp} = k_1 \hat{\mathbf{q}}_{\perp}$  and  $\mathbf{q}_{T\perp} = k_2 \hat{\mathbf{q}}_{T\perp}$ ,

$$\bar{\mathbf{T}}_{21}(\mathbf{q}_{T\perp}, \mathbf{q}_{\perp}) = t_{\parallel} \hat{\boldsymbol{\theta}}(\hat{\mathbf{q}}_T) \otimes \hat{\boldsymbol{\theta}}(\hat{\mathbf{q}}) + t_{\perp} \hat{\boldsymbol{\varphi}}(\hat{\mathbf{q}}_T) \otimes \hat{\boldsymbol{\varphi}}(\hat{\mathbf{q}}), \quad (66)$$

is the transmission dyadic. The boundary condition for the specific coherency dyadic reads as

$$\bar{\Sigma}(\mathbf{r}_M, \hat{\mathbf{q}}_T) = m^2 \frac{\cos \theta_T}{\cos \theta} \bar{\mathbf{T}}_{21}(\mathbf{q}_{T\perp}, \mathbf{q}_{\perp}) \cdot \bar{\Sigma}(\mathbf{r}_M, \hat{\mathbf{q}}) \cdot \bar{\mathbf{T}}_{21}^\dagger(\mathbf{q}_{T\perp}, \mathbf{q}_{\perp}), \quad (67)$$

where  $(\hat{\mathbf{q}}, \hat{\mathbf{q}}_T, \hat{\mathbf{n}}_0 = -\hat{\mathbf{z}})$  is a system of specular transmission directions.

### 3. Reflection and transmission matrices

To derive the expressions of the reflection and transmission matrices, we switch from the dyadic-form representations of the boundary conditions (46) and (64) to matrix-form representations [2,8,9]. In the case of reflection, we define the specific coherency column vectors in domain  $D_1$  by

$$\mathbf{J}(\mathbf{r}_M, \hat{\mathbf{q}}_R) = \frac{1}{2} \sqrt{\frac{\varepsilon_1}{\mu_0}} \begin{bmatrix} \Sigma_{\theta\theta}(\mathbf{r}_M, \hat{\mathbf{q}}_R) \\ \Sigma_{\theta\varphi}(\mathbf{r}_M, \hat{\mathbf{q}}_R) \\ \Sigma_{\varphi\theta}(\mathbf{r}_M, \hat{\mathbf{q}}_R) \\ \Sigma_{\varphi\varphi}(\mathbf{r}_M, \hat{\mathbf{q}}_R) \end{bmatrix}, \quad (68)$$

and

$$\mathbf{J}(\mathbf{r}_M, \hat{\mathbf{q}}) = \frac{1}{2} \sqrt{\frac{\varepsilon_1}{\mu_0}} \begin{bmatrix} \Sigma_{\theta\theta}(\mathbf{r}_M, \hat{\mathbf{q}}) \\ \Sigma_{\theta\varphi}(\mathbf{r}_M, \hat{\mathbf{q}}) \\ \Sigma_{\varphi\theta}(\mathbf{r}_M, \hat{\mathbf{q}}) \\ \Sigma_{\varphi\varphi}(\mathbf{r}_M, \hat{\mathbf{q}}) \end{bmatrix}, \quad (69)$$

where  $\Sigma_{\eta\mu}$  are the entries of the specific coherency dyadic  $\langle \bar{\Sigma} \rangle_S$ , and the specific intensity column vectors by

$$\mathbf{I}(\mathbf{r}_M, \cdot) = \text{DJ}(\mathbf{r}_M, \cdot) = \frac{1}{2} \sqrt{\frac{\varepsilon_1}{\mu_0}} \begin{bmatrix} \Sigma_{\theta\theta}(\mathbf{r}_M, \cdot) + \Sigma_{\varphi\varphi}(\mathbf{r}_M, \cdot) \\ \Sigma_{\theta\theta}(\mathbf{r}_M, \cdot) - \Sigma_{\varphi\varphi}(\mathbf{r}_M, \cdot) \\ -\Sigma_{\theta\varphi}(\mathbf{r}_M, \cdot) - \Sigma_{\varphi\theta}(\mathbf{r}_M, \cdot) \\ \text{j}[\Sigma_{\varphi\theta}(\mathbf{r}_M, \cdot) - \Sigma_{\theta\varphi}(\mathbf{r}_M, \cdot)] \end{bmatrix}, \quad (70)$$

where

$$D = \begin{bmatrix} 1 & 0 & 0 & 1 \\ 1 & 0 & 0 & -1 \\ 0 & -1 & -1 & 0 \\ 0 & -j & j & 0 \end{bmatrix} \quad (71)$$

is a transformation matrix. We find

$$I(\mathbf{r}_M, \hat{\mathbf{q}}_R) = \frac{1}{\pi} \int_{\Omega^+} R(\hat{\mathbf{q}}_R, \hat{\mathbf{q}}) I(\mathbf{r}_M, \hat{\mathbf{q}}) \cos \theta \, d^2 \hat{\mathbf{q}}, \quad (72)$$

where, for  $\hat{\mathbf{q}} = \hat{\mathbf{q}}(\theta, \varphi)$ , the reflection matrix  $R(\hat{\mathbf{q}}_R, \hat{\mathbf{q}})$  is given by

$$R(\hat{\mathbf{q}}_R, \hat{\mathbf{q}}) = \frac{1}{8 |\cos \theta_R| \cos \theta} \frac{|\hat{\mathbf{q}} - \hat{\mathbf{q}}_R|^4}{|\hat{\mathbf{q}} \times \hat{\mathbf{q}}_R|^4 |(\hat{\mathbf{q}} - \hat{\mathbf{q}}_R) \cdot \hat{\mathbf{z}}|^4 s^2} \times \exp\left(-\frac{t_x^2 + t_y^2}{2t_z^2 s^2}\right) M(r_{\eta\mu}). \quad (73)$$

The explicit expressions of the entries of the  $4 \times 4$  matrix  $M(r_{\eta\mu})$ ,  $\eta, \mu = \varphi, \theta$  are listed in the Appendix. The representation (51) of the reflection matrix can be also found in Ref. [12].

In the case of transmission, we define the specific coherency column vector in domain  $D_2$  by

$$J(\mathbf{r}_M, \hat{\mathbf{q}}_T) = \frac{1}{2} \sqrt{\frac{\varepsilon_2}{\mu_0}} \begin{bmatrix} \Sigma_{\theta\theta}(\mathbf{r}_M, \hat{\mathbf{q}}_T) \\ \Sigma_{\theta\varphi}(\mathbf{r}_M, \hat{\mathbf{q}}_T) \\ \Sigma_{\varphi\theta}(\mathbf{r}_M, \hat{\mathbf{q}}_T) \\ \Sigma_{\varphi\varphi}(\mathbf{r}_M, \hat{\mathbf{q}}_T) \end{bmatrix}, \quad (74)$$

and obtain the following boundary condition for the specific intensity column vector:

$$I(\mathbf{r}_M, \hat{\mathbf{q}}_T) = \frac{1}{\pi} \int_{\Omega^+} T(\hat{\mathbf{q}}_T, \hat{\mathbf{q}}) I(\mathbf{r}_M, \hat{\mathbf{q}}) \cos \theta \, d^2 \hat{\mathbf{q}}, \quad (75)$$

with the transmission matrix being given by

$$T(\hat{\mathbf{q}}_T, \hat{\mathbf{q}}) = \frac{m^3}{2 \cos \theta_T \cos \theta} \frac{|(\hat{\mathbf{q}} - m\hat{\mathbf{q}}_T) \cdot \hat{\mathbf{q}}_T|^2}{|\hat{\mathbf{q}} \times \hat{\mathbf{q}}_T|^4 |(\hat{\mathbf{q}} - m\hat{\mathbf{q}}_T) \cdot \hat{\mathbf{z}}|^4 s^2} \times \exp\left(-\frac{t_x^2 + t_y^2}{2t_z^2 s^2}\right) M(t_{\alpha\beta}). \quad (76)$$

#### 4. Final remarks

We conclude our analysis with some comments.

1. In the conventional derivation of the reflection matrix, a rough surface illuminated by a plane electromagnetic wave as in Eq. (1) is considered. In that case, the far-field pattern of the reflected field at  $P$  is (cf. Eq. (16))

$$\mathbf{E}_R^\infty(\hat{\mathbf{q}}_R) = \bar{\mathbf{A}}_{SR}(\hat{\mathbf{q}}_R, \hat{\mathbf{s}}) \cdot \mathbf{E}_0(\mathbf{r}_M), \quad (77)$$

and the specific reflection coherency dyadic is (cf. Eq. (25))

$$\bar{\Sigma}(\hat{\mathbf{q}}_R) = \frac{1}{\Delta A |\cos \theta_R|} \bar{\mathbf{A}}_{SR}(\hat{\mathbf{q}}_R, \hat{\mathbf{s}}) \cdot \bar{\mathbf{C}}_0(\hat{\mathbf{s}}) \cdot \bar{\mathbf{A}}_{SR}^\dagger(\hat{\mathbf{q}}_R, \hat{\mathbf{s}}), \quad (78)$$

where

$$\bar{\mathbf{C}}_0(\hat{\mathbf{s}}) = \mathbf{E}_0(\mathbf{r}_M) \otimes \mathbf{E}_0^*(\mathbf{r}_M) = \varepsilon_0(\hat{\mathbf{s}}) \otimes \varepsilon_0^*(\hat{\mathbf{s}}). \quad (79)$$

Using the representation  $\varepsilon_0(\hat{\mathbf{s}}) = \varepsilon_{0\theta} \hat{\boldsymbol{\theta}}(\hat{\mathbf{s}}) + \varepsilon_{0\varphi} \hat{\boldsymbol{\varphi}}(\hat{\mathbf{s}})$ , implying (say, for complex amplitudes  $\varepsilon_{0\eta}$ ,  $\eta = \varphi, \theta$ )

$$\bar{\mathbf{C}}_0(\hat{\mathbf{s}}) = \sum_{\eta, \mu = \varphi, \theta} \varepsilon_{0\eta} \varepsilon_{0\mu}^* \hat{\boldsymbol{\eta}}(\hat{\mathbf{s}}) \otimes \hat{\boldsymbol{\mu}}(\hat{\mathbf{s}}), \quad (80)$$

and putting

$$I_0(\hat{\mathbf{s}}) = \frac{1}{2} \sqrt{\frac{\varepsilon_1}{\mu_0}} \begin{bmatrix} \varepsilon_{0\theta} \varepsilon_{0\theta}^* + \varepsilon_{0\varphi} \varepsilon_{0\varphi}^* \\ \varepsilon_{0\theta} \varepsilon_{0\theta}^* - \varepsilon_{0\varphi} \varepsilon_{0\varphi}^* \\ -\varepsilon_{0\theta} \varepsilon_{0\varphi}^* - \varepsilon_{0\varphi} \varepsilon_{0\theta}^* \\ j[\varepsilon_{0\varphi} \varepsilon_{0\theta}^* - \varepsilon_{0\theta} \varepsilon_{0\varphi}^*] \end{bmatrix}, \quad (81)$$

we conclude that

$$I(\hat{\mathbf{q}}_R) = \frac{1}{\pi} R(\hat{\mathbf{q}}_R, \hat{\mathbf{s}}) I_0(\hat{\mathbf{s}}) \cos \theta_0, \quad (82)$$

with  $R(\hat{\mathbf{q}}_R, \hat{\mathbf{s}})$  as in Eq. (73).

2. The Kirchhoff approach does not account for shadowing of the incident light by the surface undulations. Attempts to include corrections for shadowing have been made in the literature by multiplying the reflection and transmission matrices by a shadowing function depending on the mean square surface slope [21,22]. The usage of a shadowing function extends the validity of the Kirchhoff approach to larger angles of incidence.
3. From Eqs. (50) and (67) we find that for a plane surface, the reflection matrix, defined by

$$I(\mathbf{r}_M, \hat{\mathbf{q}}_R) = \frac{1}{\pi} R(\hat{\mathbf{q}}_R, \hat{\mathbf{q}}) I(\mathbf{r}_M, \hat{\mathbf{q}}) \cos \theta, \quad (83)$$

is

$$R(\hat{\mathbf{q}}_R, \hat{\mathbf{q}}) = \frac{\pi}{\cos \theta} M(r_{\eta\mu}), \quad (84)$$

with  $r_{\theta\theta} = r_{\parallel}$ ,  $r_{\varphi\varphi} = r_{\perp}$ , and  $r_{\theta\varphi} = r_{\varphi\theta} = 0$ , while the transmission matrix, defined by

$$I(\mathbf{r}_M, \hat{\mathbf{q}}_T) = \frac{1}{\pi} T(\hat{\mathbf{q}}_T, \hat{\mathbf{q}}) I(\mathbf{r}_M, \hat{\mathbf{q}}) \cos \theta \quad (85)$$

is

$$T(\hat{\mathbf{q}}_T, \hat{\mathbf{q}}) = \pi m^3 \frac{\cos \theta_T}{\cos^2 \theta} M(t_{\eta\mu}), \quad (86)$$

with  $t_{\theta\theta} = t_{\parallel}$ ,  $t_{\varphi\varphi} = t_{\perp}$ , and  $t_{\theta\varphi} = t_{\varphi\theta} = 0$ .

4. Letting  $\cos \Theta = \hat{\mathbf{q}} \cdot \hat{\mathbf{q}}_R = \cos \theta \cos \theta_R + \sin \theta \sin \theta_R \cos(\varphi - \varphi_R)$  be the cosine of the scattering angle, and defining

$$\cos \beta = \frac{\cos \theta - \cos \theta_R}{\sqrt{2(1 - \cos \Theta)}}, \quad (87)$$

we obtain an equivalent representation for the reflection matrix:

$$R(\hat{\mathbf{q}}_R, \hat{\mathbf{q}}) = \frac{1}{8 |\cos \theta_R| \cos \theta} \frac{1}{\sin^4 \Theta \cos^4 \beta s^2} \times \exp\left(-\frac{1 - \cos^2 \beta}{2s^2 \cos^2 \beta}\right) M(r_{\eta\mu}). \quad (88)$$

Similarly, defining

$$\cos \beta = \frac{\cos \theta - m \cos \theta_T}{\sqrt{1 + m^2 - 2m \cos \Theta}}, \quad (89)$$

with  $\cos \Theta = \hat{\mathbf{q}} \cdot \hat{\mathbf{q}}_T$ , we obtain an equivalent representation for the transmission matrix:

$$T(\hat{\mathbf{q}}_T, \hat{\mathbf{q}}) = \frac{m^3}{2 \cos \theta_T \cos \theta} \frac{(m - \cos \Theta)^2}{\sin^4 \Theta (\cos \theta - m \cos \theta_T)^4 s^2} \times \exp\left(-\frac{1 - \cos^2 \beta}{2s^2 \cos^2 \beta}\right) M(t_{\eta\mu}). \quad (90)$$

The relations (88) and (90) are practical formulas for computing the reflection and transmission matrices for a rough surface and coincide with those of the phenomenological approach (based on a facet model for the rough surface) described in [18]. It should be pointed out that in [18], the Fresnel reflection and transmission coefficients are replaced by the corresponding reflection and transmission matrices, which in turn, are multiplied by the rotation matrices corresponding to the transformation of the radiance vectors from the scattering to the meridian planes. In our derivation, these transformations are already encapsulated in the matrices  $M(r_{\eta\mu})$  and  $M(t_{\eta\mu})$ .

5. In the scalar radiative transfer, the quantities of interest are the first element of the specific intensity column vector (the specific intensity) and the (1,1) element of the reflection (transmission) matrix. This simplification is widely used when the medium is illuminated by unpolarized light and only the specific intensity of the multiply scattered light needs to be computed. Using

$$\sum_{\eta,\mu=\varphi,\theta} r_{\eta\mu}^2 = \frac{r_{\parallel}^2 + r_{\perp}^2}{2} \sin^4 \Theta, \quad (91)$$

in Eq. (88) gives

$$[\mathbf{R}(\hat{\mathbf{q}}_{\mathbf{R}}, \hat{\mathbf{q}})]_{11} = \frac{1}{8|\cos\theta_{\mathbf{R}}|\cos\theta\cos^4\beta s^2} \times \exp\left(-\frac{1-\cos^2\beta}{2s^2\cos^2\beta}\right) \frac{r_{\parallel}^2 + r_{\perp}^2}{2}, \quad (92)$$

while using

$$\sum_{\eta,\mu=\varphi,\theta} t_{\eta\mu}^2 = \frac{t_{\parallel}^2 + t_{\perp}^2}{2} \sin^4 \Theta, \quad (93)$$

in Eq. (90) yields

$$[\mathbf{T}(\hat{\mathbf{q}}_{\mathbf{R}}, \hat{\mathbf{q}})]_{11} = \frac{m^3}{2\cos\theta_{\mathbf{T}}\cos\theta} \frac{(m - \cos\Theta)^2}{(\cos\theta - m\cos\theta_{\mathbf{T}})^4 s^2} \times \exp\left(-\frac{1-\cos^2\beta}{2s^2\cos^2\beta}\right) \frac{t_{\parallel}^2 + t_{\perp}^2}{2}. \quad (94)$$

Note that the relations (92) and (94) can be found in Ref. [18].

## Appendix A

The entries of the  $4 \times 4$  matrix  $\mathbf{M}(r_{\eta\mu})$ ,  $\eta, \mu = \varphi, \theta$  are given by

$$[\mathbf{M}]_{11} = \frac{1}{2} (|r_{\theta\theta}|^2 + |r_{\theta\varphi}|^2 + |r_{\varphi\theta}|^2 + |r_{\varphi\varphi}|^2), \quad (95)$$

$$[\mathbf{M}]_{12} = \frac{1}{2} (|r_{\theta\theta}|^2 - |r_{\theta\varphi}|^2 + |r_{\varphi\theta}|^2 - |r_{\varphi\varphi}|^2), \quad (96)$$

$$[\mathbf{M}]_{13} = -\text{Re}(r_{\theta\theta}r_{\theta\varphi}^* + r_{\varphi\varphi}r_{\varphi\theta}^*), \quad (97)$$

$$[\mathbf{M}]_{14} = -\text{Im}(r_{\theta\theta}r_{\theta\varphi}^* - r_{\varphi\varphi}r_{\varphi\theta}^*), \quad (98)$$

$$[\mathbf{M}]_{21} = \frac{1}{2} (|r_{\theta\theta}|^2 + |r_{\theta\varphi}|^2 - |r_{\varphi\theta}|^2 - |r_{\varphi\varphi}|^2), \quad (99)$$

$$[\mathbf{M}]_{22} = \frac{1}{2} (|r_{\theta\theta}|^2 - |r_{\theta\varphi}|^2 - |r_{\varphi\theta}|^2 + |r_{\varphi\varphi}|^2), \quad (100)$$

$$[\mathbf{M}]_{23} = -\text{Re}(r_{\theta\theta}r_{\theta\varphi}^* - r_{\varphi\varphi}r_{\varphi\theta}^*), \quad (101)$$

$$[\mathbf{M}]_{24} = -\text{Im}(r_{\theta\theta}r_{\theta\varphi}^* + r_{\varphi\varphi}r_{\varphi\theta}^*), \quad (102)$$

$$[\mathbf{M}]_{31} = -\text{Re}(r_{\theta\theta}r_{\varphi\theta}^* + r_{\varphi\varphi}r_{\theta\varphi}^*), \quad (103)$$

$$[\mathbf{M}]_{32} = -\text{Re}(r_{\theta\theta}r_{\varphi\theta}^* - r_{\varphi\varphi}r_{\theta\varphi}^*), \quad (104)$$

$$[\mathbf{M}]_{33} = \text{Re}(r_{\theta\theta}r_{\varphi\varphi}^* + r_{\theta\varphi}r_{\varphi\theta}^*), \quad (105)$$

$$[\mathbf{M}]_{34} = \text{Im}(r_{\theta\theta}r_{\varphi\varphi}^* + r_{\theta\varphi}r_{\varphi\theta}^*), \quad (106)$$

$$[\mathbf{M}]_{41} = -\text{Im}(r_{\varphi\theta}r_{\theta\theta}^* + r_{\varphi\varphi}r_{\theta\varphi}^*), \quad (107)$$

$$[\mathbf{M}]_{42} = -\text{Im}(r_{\varphi\theta}r_{\theta\theta}^* - r_{\varphi\varphi}r_{\theta\varphi}^*), \quad (108)$$

$$[\mathbf{M}]_{43} = \text{Im}(r_{\varphi\varphi}r_{\theta\theta}^* - r_{\theta\varphi}r_{\varphi\theta}^*), \quad (109)$$

$$[\mathbf{M}]_{44} = \text{Re}(r_{\varphi\varphi}r_{\theta\theta}^* - r_{\theta\varphi}r_{\varphi\theta}^*). \quad (110)$$

For practical applications, it is important to note that  $r_{\eta\mu} = r_{\eta\mu}(\theta, \theta_{\mathbf{R}}, \varphi - \varphi_{\mathbf{R}})$ , and so, that an azimuthal expansion of  $\mathbf{M}(r_{\eta\mu})$  in terms of the relative azimuthal angle  $\varphi - \varphi_{\mathbf{R}}$  is appropriate. This becomes apparent from the explicit expressions of the quantities which enter in Eqs. (32)–(35), namely

$$\cos\theta_{\mathbf{L}0} = \sqrt{\frac{1 - \cos\Theta}{2}}, \quad (111)$$

$$\hat{\boldsymbol{\varphi}}(\hat{\mathbf{q}}) \cdot \hat{\mathbf{q}}_{\mathbf{R}} = -\sin\theta_{\mathbf{R}} \sin(\varphi - \varphi_{\mathbf{R}}), \quad (112)$$

$$\hat{\boldsymbol{\theta}}(\hat{\mathbf{q}}) \cdot \hat{\mathbf{q}}_{\mathbf{R}} = \cos\theta \sin\theta_{\mathbf{R}} \cos(\varphi - \varphi_{\mathbf{R}}) - \sin\theta \cos\theta_{\mathbf{R}}, \quad (113)$$

$$\hat{\boldsymbol{\varphi}}(\hat{\mathbf{q}}_{\mathbf{R}}) \cdot \hat{\mathbf{q}} = \sin\theta \sin(\varphi - \varphi_{\mathbf{R}}), \quad (114)$$

$$\hat{\boldsymbol{\theta}}(\hat{\mathbf{q}}_{\mathbf{R}}) \cdot \hat{\mathbf{q}} = \cos\theta_{\mathbf{R}} \sin\theta \cos(\varphi - \varphi_{\mathbf{R}}) - \sin\theta_{\mathbf{R}} \cos\theta. \quad (115)$$

The matrix  $\mathbf{M}(t_{\eta\mu})$  has the same property. The scalars  $\hat{\boldsymbol{\eta}}(\hat{\mathbf{q}}) \cdot \hat{\mathbf{q}}_{\mathbf{T}}$  and  $\hat{\boldsymbol{\eta}}(\hat{\mathbf{q}}_{\mathbf{T}}) \cdot \hat{\mathbf{q}}$  are as in Eqs. (112)–(115) but with  $\theta_{\mathbf{T}}$  and  $\varphi_{\mathbf{T}}$  replacing  $\theta_{\mathbf{R}}$  and  $\varphi_{\mathbf{R}}$ , respectively, while the cosine of the local incident angle  $\theta_{\mathbf{L}0}$  is given by

$$\cos\theta_{\mathbf{L}0} = \frac{m \cos\Theta - 1}{\sqrt{1 + m^2 - 2m \cos\Theta}}. \quad (116)$$

## References

- [1] Mishchenko MI, Dlugach JM, Yurkin MA, Bi L, Cairns B, Liu L, Panetta RL, Travis LD, Yang P, Zakharova NT. First-principles modeling of electromagnetic scattering by discrete and discretely heterogeneous random media. *Phys Rep* 2016;632:1–75.
- [2] Mishchenko MI. *Electromagnetic scattering by particles and particle groups: an introduction*. Cambridge, UK: Cambridge University Press; 2014. [https://www.giss.nasa.gov/staff/mmishchenko/publications/Book\\_4.pdf](https://www.giss.nasa.gov/staff/mmishchenko/publications/Book_4.pdf)
- [3] Mishchenko MI. Directional radiometry and radiative transfer: the convoluted path from centuries-old phenomenology to physical optics. *J Quant Spectrosc Radiat Transfer* 2014;146:4–33.
- [4] Soubret A, Berginc G. Electromagnetic wave scattering from a random layer with rough interfaces I: Coherent field. *arXiv:physics/0312133*.
- [5] Soubret A, Berginc G. Electromagnetic wave scattering from a random layer with rough interfaces II: Diffusive intensity. *arXiv:physics/0312136*.
- [6] Mudaliar S. Remote sensing of layered random media using the radiative transfer theory. *Radio Sci* 2013;48:535–46.
- [7] Apresyan LA, Kravtsov Yu A. *Radiation transfer. Statistical and wave aspects*. Basel: Gordon and Breach; 1996.
- [8] Mishchenko MI. Vector radiative transfer equation for arbitrarily shaped and arbitrarily oriented particles: a microphysical derivation from statistical electromagnetics. *Appl Opt* 2002;41:7114–34.
- [9] Mishchenko MI, Travis LD, Lacis AA. *Multiple scattering of light by particles: radiative transfer and coherent backscattering*. Cambridge: Cambridge University Press; 2006.
- [10] Tsang L, Kong JA, Shin RT. *Theory of microwave remote sensing*. New York: Wiley; 1985.



- [11] Tsang L, Kong JA. Scattering of electromagnetic waves. Advanced topics. New York: Wiley; 2001.
- [12] Mishchenko MI, Travis LD. Satellite retrieval of aerosol properties over ocean using polarization as well as intensity of reflected sunlight. *J Geophys Res* 1997;102:16989–7013.
- [13] Cox C, Munk W. Statistics of the sea surface derived from sun glitter. *J Mar Res* 1954;13:198–227.
- [14] Cox C, Munk W. Measurement of the roughness of the sea surface from photographs of the sun's glitter. *J Opt Soc Am* 1954;44:838–50.
- [15] Nakajima T, Tanaka M. Effect of wind-generated waves on the transfer of solar radiation in the atmosphere–ocean system. *J Quant Spectrosc Radiat Transfer* 1983;29:521–37.
- [16] Jin Z, Stamnes K. Radiative transfer in nonuniformly refracting layered media: atmosphere–ocean system. *Appl Opt* 1994;33:431–42.
- [17] Jin Z, Charlock TP, Rutledge K, Stamnes K, Wang Y. Analytical solution of radiative transfer in the coupled atmosphere–ocean system with a rough surface. *Appl Opt* 2006;45:7443–55.
- [18] Zhai PW, Hu Y, Chowdhary J, Trepte CR, Lucker PL, Josset DB. A vector radiative transfer model for coupled atmosphere and ocean systems with a rough interface. *J Quant Spectrosc Radiat Transfer* 2010;111:1025–240.
- [19] Beckmann P, Spizzichino A. The scattering of electromagnetic waves from rough surfaces. Artech House, Norwood: Massachusetts; 1987.
- [20] Voronovich AG. Wave scattering from rough surfaces. Berlin: Springer-Verlag; 1999.
- [21] Smith BG. Geometrical shadowing of a random rough surface. *IEEE Trans Antennas Propag* 1967;15:668–71.
- [22] Sancer MI. Shadow-corrected electromagnetic scattering from a randomly rough surface. *IEEE Trans Antennas Propag* 1969;17:577–85.